International Journal of Naval Architecture and Ocean Engineering 11 (2019) 828–834

Contents lists available at ScienceDirect

International Journal of Naval Architecture and Ocean Engineering

journal homepage: http://www.journals.elsevier.com/international-journal-of-naval-architecture-and-ocean-engineering/

Thrust estimation of a flapping foil attached to an elastic plate using multiple regression analysis

Rupesh Kumar, Hyunkyoung Shin*

School of Naval Architecture and Ocean Engineering, University of Ulsan, 93 Daehak-ro, Namgu, Ulsan, 44610, Republic of Korea

ARTICLE INFO

Article history:
Received 31 July 2018
Received in revised form
20 November 2018
Accepted 19 February 2019
Available online 20 February 2019

Keywords:
Flapping foil
Regression analysis
Station keeping
Thrust
Elastic plate

ABSTRACT

Researchers have previously proven that the flapping motion of the hydrofoil can convert wave energy into propulsive energy. However, the estimation of thrust forces generated by the flapping foil placed in waves remains a challenging task for ocean engineers owing to the complex dynamics and uncertainties involved. In this study, the flapping foil system consists of a rigid NACA0015 section undergoing harmonic flapping motion and a passively actuated elastic flat plate attached to the leading edge of the rigid foil. We have experimentally measured the thrust force generated due to the flapping motion of a rigid foil attached to an elastic plate in a wave flume, and the effects of the elastic plates have been discussed in detail. Furthermore, an empirical formula was introduced to predict the thrust force of a flapping foil based on our experimental results using multiple regression analysis.

1. Introduction

In nature, birds, fish, and insects maneuver using their wings or tails. That is, maneuvering forces are generated by the flapping motion of their foil-shaped wings, fins or tails, which produce thrust by means of a direct conversion from fluid flow to propulsive energy. This concept has inspired numerous researchers to improve the propulsive and maneuvering abilities of man-made devices in air and water. In 1895, Linden (1895) built a 13 ft long boat which moved against the waves at three to four miles per hour, powered purely by the thrust generated from two underwater steel plates using wave energy. In 1966, Gause (1966) filed his first patent for a wave powered boat, he attached three flexible fins to a 34 ft boat and attained a maximum speed of 5 mph using energy of the waves. Thereafter, several naval researchers, such as Terao (1982), Jakobsen (1981), and Isshiki (1994), had reported very interesting experimental results using flapping foils. According to these reports, a model ship could move against incoming waves with the aid of flapping foils alone and the ship speed was dependent on the wave conditions, a phenomenon known as “wave devouring propulsion.” It was also found that the flapping foil propulsion system has higher efficiency, lower noise, better maneuverability and control systems (Yu et al., 2004; Fish, 2013). Subsequently, the application of flapping foil as an auxiliary propulsor near the free surface have been studied (Bøckmann and Steen, 2014; Filippas and Belibassakis, 2014). Read (Read et al., 2003) and Hover (Hover et al., 2004) reported on the forces on flapping foils for propulsion and maneuvering, and the effects of the attack angle on flapping foil propulsion, respectively.

In 1958, Ulysses (1958) experimented with a boat that had four fixed fins and found that the fins were capable of not only increasing the thrust but also reducing pitch boat motion. These foils are referred to as “anti-pitching fins.” Subsequently, researchers changed the foil location to obtain other advantages, such as anti-rolling (Evangelos, 2015). Afterwards, many innovative ideas were presented on flapping flexible foils (Liu et al., 2018). Studies on the chord-wise flexibility of a flapping foil were presented (Prempraneerach et al., 2003). They found that the efficiency of the foil was increased due to the chord-wise flexibility of the foil compared to rigid foils. Subsequently, researchers had experimented with span-wise flexibility (Zhou et al., 2017). It was found that the span-wise flexibility could improve the propulsive efficiency by adjusting the motions and flexibility parameters. In 2017, A new propulsion system using flapping foils was presented (Ripon and JMKG, n.d), he used two flapping foils that flapped together in and out of phase over angles of 180°, which could generate lift and forward thrust with better efficiency compared to

* Corresponding author.
E-mail addresses: rupesh7243@gmail.com (R. Kumar), hkshin@ulsan.ac.kr (H. Shin).
Peer review under responsibility of Society of Naval Architects of Korea.

https://doi.org/10.1016/j.ijnaoe.2019.02.006

Nomenclature

S	Span of hydrofoil (cm)
L	Length of elastic plate (cm)
T	Thrust (N)
Lw	Wavelength (m)
ω	Wave frequency (rad/s)
A_{EP}	Area of elastic plate (cm^2)
C	Chord of hydrofoil (cm)
B	Breadth of elastic plate (cm)
K	Wave number
H	Wave height (mm)
D	Water depth (cm)
A_F	Area of hydrofoil (cm^2)

screw propellers. Recently, Liu (Liu et al., 2017) presented a research study on the flapping foil with a plate connected to the trailing edge of the foil. He used a spring in the tail to make it flexible and found that an oscillating plate connected to the trailing edge of the flapping foil could enhance the performance of the system.

Despite extensive studies on the flapping foil dynamics, the experimental measurements of the thrust force without forward motion has drawn relatively less scientific interest. Most of the researchers have studied the heave and pitch motion of the foil against incoming free stream (Xu et al., 2017; Blondeaux et al., 2005) or the foil itself moving in steady forward motion (Liu et al., 2017; Xie et al., 2016; Belibassakis et al., 2015). Also, fewer studies have been carried out on the flapping foil extracting energy from the free surface waves. Silva (Silva and Yamaguchi, 2012) numerically studied the performance of a two-dimensional rigid foil in gravity waves. The investigated results explained that when some key parameters are correctly maintained, the flapping foil could increase its performance in waves. Therefore, from the previous literature it can be summarized that a flexible foil flapping near the free surface could be more efficient for the generation of thrust forces. However, the measurement of flexibility has not drawn much interests of the researchers so far. Also, when we think of stationkeeping of a floater in waves using flapping foils, the measurement of thrust forces generated by a flapping foil in waves without any forward velocity becomes important.

In this study, we carried out experiments with a rigid foil connected to a flexible plate to its leading edge in surface gravity waves and the thrust forces generated by the flapping motion of the foil were recorded. We also observed experimentally that a minor change in the elastic plate attached to the leading edge of the foil can have a significant effect on the thrust generation of the flapping foil. Furthermore, based on our experimental results, we introduced an empirical formula for the thrust estimation of the flapping foil in regular waves using multiple regression analysis and the empirical formula was verified by other experiments in a widetank with different water depth.

2. Model test

2.1. Model preparation

The foil used for all the experiments was rectangular with a constant NACA0015 section, a chord of 8 cm, and a span of 20 cm. It was rigid, neutrally buoyant, and constructed of acrylic. The elastic plate was also rectangular with a constant thickness of 0.1 cm and made of polyethylene. The flat plate was attached to the leading edge of the rigid foil, as displayed in Fig. 1. The dimensions of the hydrofoil remained constant throughout the experiments. However, the dimensions of the elastic plate varied as shown in Table 1(a) and Table 1(b). Where L represents the length of elastic plates, B represents the breadth of elastic plates, C and S represent chord and span of the hydrofoil respectively. The plan used for carrying out experiments is shown in detail in Fig. 2 where a rigid hydrofoil was experimented with three different lengths of elastic plates and each length of elastic plates attached with the hydrofoil was experimented with the three different breadths of the elastic plates. Therefore, total nine models were prepared for the experiments and each model consists of the same hydrofoil.

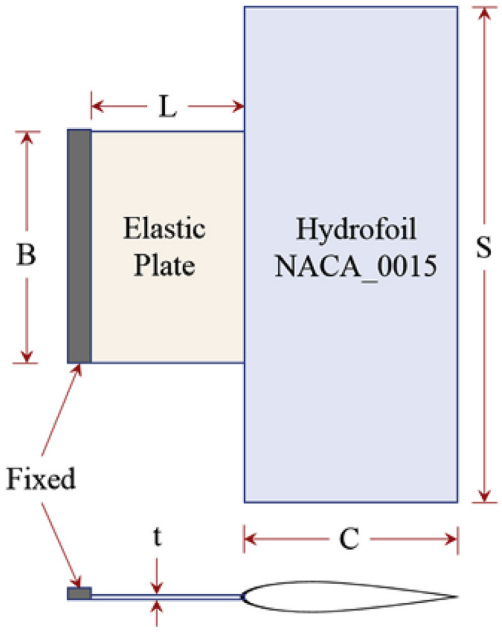

Fig. 1. Flapping foil.

Table 1a
Lengths of elastic plate.

Length	L1	L2	L3
L/C	1.125	0.750	0.375

Table 1b
Breadths of elastic plate.

Breadth	B1	B2	B3
B/S	1.0	0.5	0.2

2.2. Load cases

Flapping foil experiments were performed for the twenty-four wave conditions for each set of the models, as shown in the experimental plan of Fig. 2. Table 2(a) shows eight load cases for wavelengths (Lw) in the range of 0.25 m–3.69 m. These wavelengths are repeated for three wave heights (H), as shown in Table 2(b). Therefore, 24 load case experiments were carried out in total for each set of the models.

2.3. Experimental setup

The flapping foil experiments were carried out in a wave flume in the Ocean Engineering Lab, University of Ulsan. The flume was

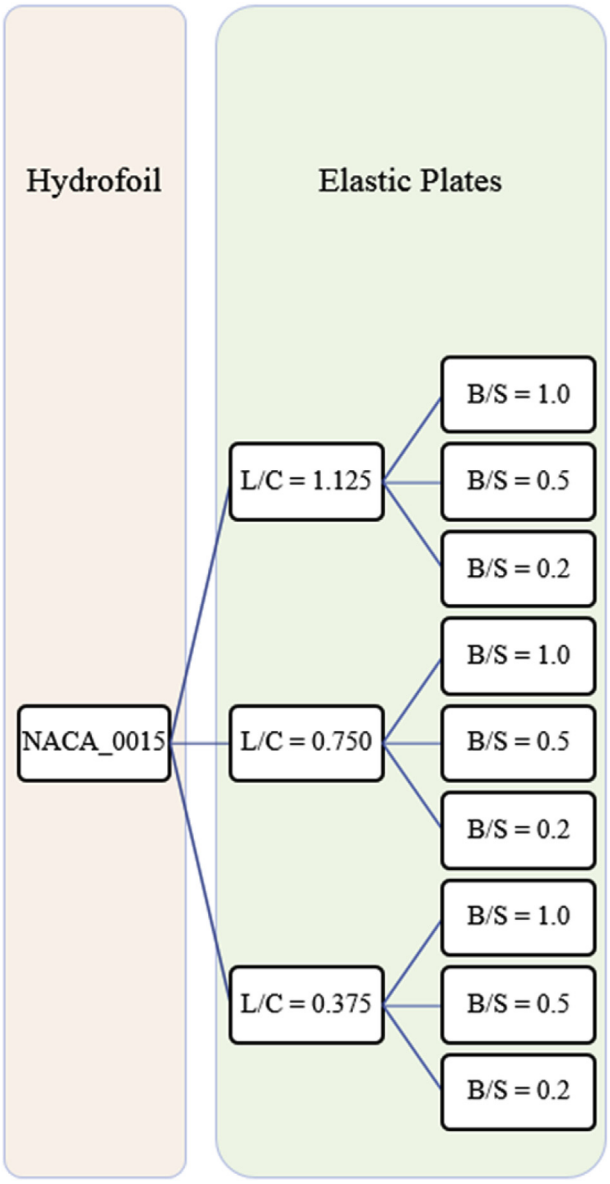

Fig. 2. Experiment plan.

Table 2a
Load cases.

Serial Number	RPM	Period (s)	Status	K	ω (rad/s)	Lw (m)
1	10	2.0	Finite	1.7	3.13	3.69
2	15	1.4	Finite	2.7	4.63	2.30
3	20	1.0	Finite	4.2	6.22	1.49
4	25	0.8	Finite	6.2	7.75	1.01
5	30	0.7	Deep	8.7	9.24	0.72
6	35	0.6	Deep	12.0	10.86	0.52
7	40	0.5	Deep	15.5	12.32	0.41
8	50	0.4	Deep	25.2	15.71	0.25

35 m long, 0.5 m wide, and 0.6 m deep. A wave-maker was located at one end of the tank to generate the desired waves. At the other end of the tank, a wave absorbing beach was used to dissipate the wave energy and reduce wave reflection. The water depth and submergence of the foil were, respectively, equal to 0.4 m and 0.05 m and were unchanged during the experiments.

Table 2b
Wave heights (H).

Serial Number	H(mm)
1	10
2	20
3	30

A wave probe was mounted on the fixed frame of a tank, which was positioned 3 m away from the wave paddle. The wave probe was able to measure the water level fluctuations to the nearest 0.5 mm. The diameter of the probe wire was 0.3 cm and its placement in the water before the flapping foil did not cause any significant modification to the wave field. A load cell was mounted on the fixed frame of the tank, which was positioned 0.2 m from the wave probe. The load cell was able to measure the thrust forces in the x-direction of the wave flume as shown in Fig. 3 (Lee et al., 2017). The maximum capacity of the load cell was 10 N and was changed to 0.2 N to increase the accuracy of the measurements. The load cell was set to produce 100 observations per second. In general, the load cell was used to record the thrust force of the flapping foil, whereby the flapping foil was attached to the load cell through a slender rigid column. Therefore, a thrust force generated by a flapping foil was experienced by the slender rigid column, which transferred the thrust force to the load cell to record it. Thrust forces measured along the direction opposite to the incident wave were recorded as positive, and the forces measured along the direction of the wave, as negative. The experimental setup is displayed in Fig. 3.

2.4. Experimental results

Fig. 4 shows the thrust forces in time domain generated by a flapping foil during experiments. The positive and negative thrusts were obtained for each stroke of the flapping motion of foil and mean value was observed as the thrust force for the regression analysis.

Fig. 5 presents the experimental results of the flapping foil. Additionally, a comparison of the thrust generation of a flapping foil for three different wave heights (10 mm, 20 mm and 30 mm) is displayed. Table 1(a) and Table 1(b) define L1, L2, L3 and B1, B2, B3 respectively.

2.5. Effects of the length of elastic plate

The effectiveness of the elastic plate was largely dependent on the slenderness ratio (L/B) and the area of the elastic plates (A_{EP}) as shown in Table 3. The lengths (L) of the elastic plate have significant effects on the thrust estimation of the flapping foil. As shown in Fig. 6, when the breadth is fixed to B1, the foil with larger length 'L1' could displace more from its original position and would have larger oscillating period. Thus, it is more suitable for long waves. On the other hand, when the length of the elastic plate is smaller, the foil could have a smaller deflection and oscillating period thus, is suitable for the short waves. Also, the low slenderness ratio with bigger area generates bigger thrust therefore, in case of B1 Fig. 6, L2 generates bigger thrust compared to L1 and L3. The effects of slenderness ratio could be observed when the breadth of elastic plate was fixed to B2 as well. In case of B3, L1 and L2 show peculiar trends because B3 was the smallest breadth and the slenderness ratios were very high as 2.25 and 1.50 respectively. It means, elastic plates were very much flexible and only suitable for very long waves.

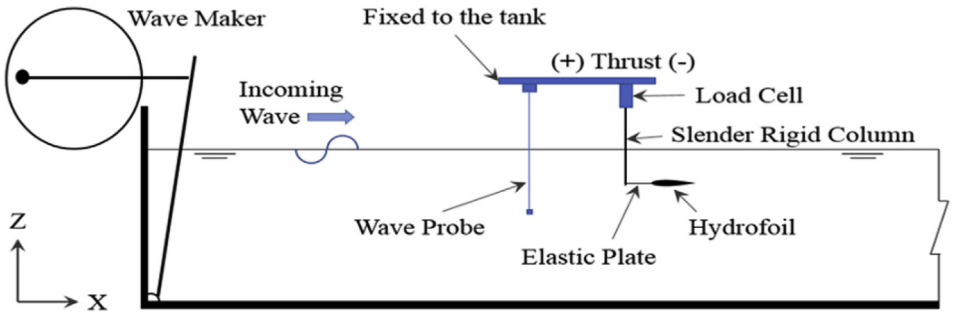

Fig. 3. Experimental setup in a wave flume, UOU.

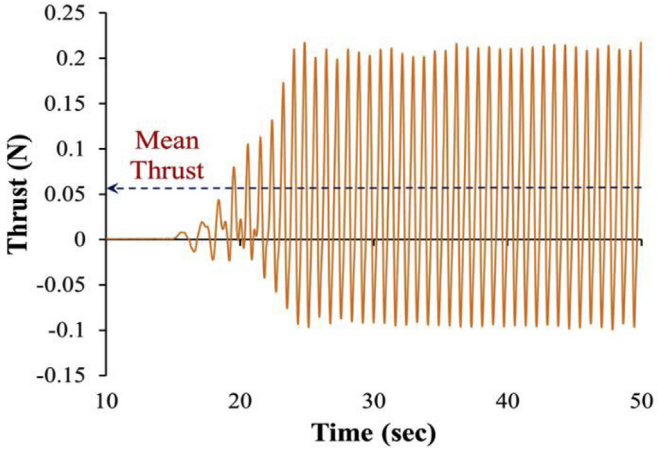

Fig. 4. Thrust measurement using load cell.

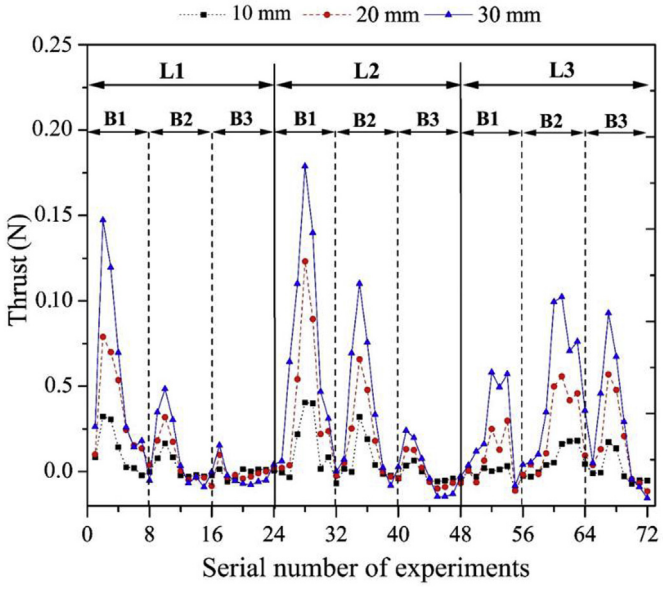

Fig. 5. Experimental results.

2.6. Effects of the breadth of elastic plate

The breadth (B) of the elastic plate also has a significant effect on the thrust estimation of the flapping foil. When the breadth is larger, the foil could not displace more from its neutral position owing to an increase in the rigidity of the elastic plate and oscillate with the shorter time period. Thus, it was more suitable for middle-sized and short waves, as shown in Fig. 7. On the other hand, when the breadth of the elastic plate was smaller, it was more suitable for long waves due to decreased rigidity of the elastic plates.

Table 3
Slenderness ratio and area of the elastic plates.

Length	Breadth	L/B	A_{EP} (cm^2)
L1	B1	0.45	180
	B2	0.90	90
	B3	2.25	36
L2	B1	0.30	120
	B2	0.60	60
	B3	1.50	24
L3	B1	0.15	60
	B2	0.30	30
	B3	0.75	12

In general, the bigger area of the elastic plate generates bigger thrust as shown in L1 and L2 case of Fig. 7. Where B1 is bigger than B2 and B3 thus B1 generates bigger thrust followed by B2 and B3. However, in case of L3, B2 and B3 generates bigger thrust than B1due to very low slenderness ratio (L/B = 0.15).

Therefore, it can be concluded that the slenderness ratio of the elastic plate (E = 1 GPa, t = 0.1 cm) should be (0.2 < L/B < 1.0) for the effective thrust generation of flapping foil in regular waves.

3. Procedure for estimating thrust force

3.1. Dimensional analysis

To proceed with the multiple regression analysis of the experimental data, we needed to estimate the non-dimensional numbers. Thus, we opted for a dimensional analysis of the geometrical, environmental, and material properties of the flapping foil experiments.

The thrust of the flapping foil depends on the parameters listed in Table 4. Where length of elastic plate (L) and breadth of elastic plate (B) are geometric properties of the flapping foil.

Mass density (ρ), acceleration due to gravity (g), wave height (H), wave length (L_w), dynamic viscosity of water (μ) and added pitch moment of elastic plate (I_a) represent environmental properties and material properties for the dimensional analysis was represented by the flexural rigidity of elastic plates (EI).

The added pitch moment of elastic plates (I_a) was obtained from the pitch wave radiation of the elastic plates in gravity waves using UOU in-house code. The elastic modulus of the elastic plates (E) was obtained from a small test carried out in the lab. We used an elastic plate of length 14 cm and breadth 8 cm which was clamped at one end like a cantilever beam and applied loads varying from 100 N to 400 N on the free end of the elastic plate and recorded the deflection for all the applied loads. This experiment was repeated two

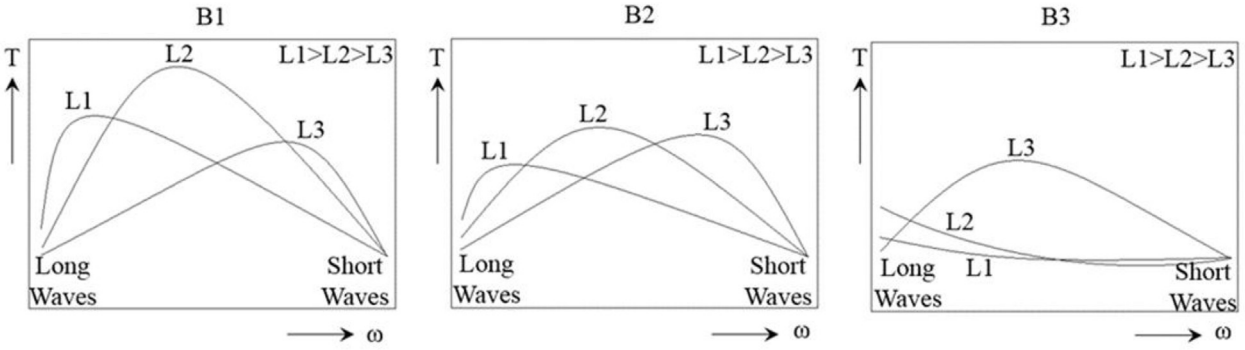

Fig. 6. Effects of the length of elastic plate on thrust force.

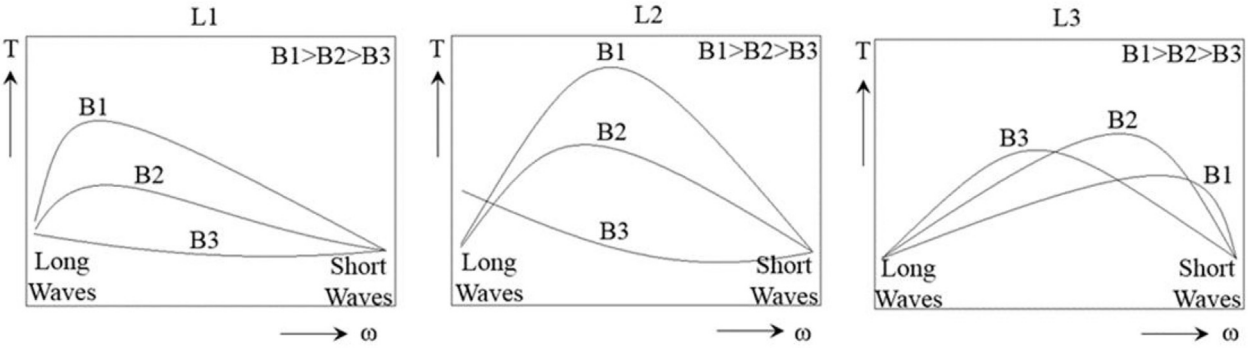

Fig. 7. Effects of the breadth of elastic plate on thrust force.

Table 4
Parameters that influence the thrust force.

Sl. No.	Parameters	Dimension
1	Mass density (ρ)	$M\,L^{-3}$
2	Breadth of elastic plate (B)	L
3	Length of elastic plate (L)	L
4	Acceleration due to gravity (g)	$L\,T^{-2}$
5	Wave Height (H)	L
6	Wave Length (L_w)	L
7	Fluid viscosity (μ)	$M\,L^{-1}\,T^{-1}$
8	Flexural rigidity of elastic plate (EI)	$M\,L^{3}\,T^{-2}$
9	Added pitch moment of elastic plate (I_a)	$M\,L^{2}$

more times and average value was used for the estimation of the elastic modulus of plates (E = 1.072 GPa) using the beam theory formula for the cantilever beam. Further, the wave orbital velocity was obtained from the multiplications of incoming wave frequency (ω) and amplitude (H/2). Density of water was assumed as 1000 kg/m^3. The dynamic viscosity of the fresh water (μ) at 25^0c was assumed as 8.9×10^{-4} *Pa.s*. Area of Foil (A_F) and water depth (D) were unchanged through the process of thrust estimation.

Dimensional Analysis:

$$T \propto \rho^a B^b L^C g^d H^e (L_w)^f \mu^g (EI)^h (I_a)^i \tag{1}$$

Total number of variables (m) = 10.
Total number of fundamental dimensions (n) = 3.
Total number of non-dimensional quantities = m - n = 7

$$T = \rho g L^3 f\left\{\left(\frac{B}{L}\right)^b \left(\frac{L_w}{L}\right)^C \left(\frac{H}{L_w}\right)^e \left(\frac{\mu}{\rho L (gL)^{0\cdot5}}\right)^g \left(\frac{EI}{\rho g L^5}\right)^h \left(\frac{I_a}{\rho L^5}\right)^i\right\} \tag{2}$$

$$\frac{T}{\frac{1}{2}\rho L^2 V^2} = f\left\{\left(\frac{L}{B}\right)^j \left(\frac{gL}{V^2}\right)^p \left(\frac{H}{L_w}\right)^e \left(\frac{\mu}{\rho V L}\right)^q \left(\frac{EI}{\rho V^2 L^4}\right)^h \left(\frac{I_a}{\rho L^5}\right)^i\right\} \tag{3}$$

Where;

$$V = \frac{\omega H}{2} \tag{4}$$

From dispersion relation,

$$\frac{\omega^2}{g} = \frac{2\pi}{L_w} \tanh\left(\frac{2\pi}{L_w} D\right) \tag{5}$$

Where, Eq. (1) shows that the thrust force generated by a flapping foil in waves was directly proportional to the variables shown in Table 4. Eq. (2) shows the arrangement of variables in non-dimensional form using Buckingham-pi theorem. Eq. (3) rearranges the dimensionless terms by introducing the velocity into it that shows the total 7 non-dimensional quantities that was reduced from the total 10 numbers of variables. Also, these 7 non-dimensional quantities will be carried for the regression analysis. Eq. (4) explains the velocity in which wave frequency (ω) was obtained from the dispersion relation in shallow water for each wave lengths in a given water depth as shown in Eq. (5). In deep water case, the tangent hyperbolic goes very near to 1.

3.2. Multiple regression analysis

The thrust force of a flapping foil depends on the elastic plate and wave conditions. Therefore, the thrust coefficient is considered as a dependent variable, while the slenderness ratio, wave slope,

Table 5
Variables for multiple regression analysis.

Sl. No.	Variables	Short Notation	Mathematical Expression
1	Thrust coefficient	Ct	$T/0.5\rho(A_F)V^2$
2	Slenderness ratio of elastic plate	Slr	L/B
3	Wave slope	Ws	H/Lw
4	Froude number	Fn	$V/\sqrt{gL}$
5	Reynolds number	Rn	$VL\rho/\mu$
6	Elastic plate number	Ep	$EI/\rho V^2(A_{EP})^2$
7	Added mass number	Ad	$Ia/\rho L^5$

Froude number, Reynolds number, elastic plate number, and added mass number are independent variables. The short notations and mathematical presentations of these variables can be found in Table 5. We made sure that all the independent variables were correlated individually with the dependent variable and had a p-value that was smaller than 0.05. Thus, the dependent variable (C_t) can be written as a function of all the independent functions as shown in Eq. (6).

$$Ct = f\{Slr, Ws, Rn, Fn, Ep, Ad\} \quad (6)$$

Multiple regression analysis was carried out by using the results of the model tests, as displayed in Fig. 5. Once the independent variables are finalized and applied to the multiple regression analysis, the multiple regression model yields a value of 92% (R = 0.92), which is very stable because the difference between them is small. Table 6 shows each coefficient, the standard errors, t-statistics, p-values, and the lower and the upper 95% values. The explanation provided by the multiple regression model is supported because all the p-values are smaller than the significance level of 0.05.

It was found that the Fn and Rn values were strongly correlated. Thus, to avoid multicollinearity, Rn was eliminated from the regression analysis. Because, the foil was flapping owing to orbital velocity of surface waves that was dominated by gravity forces. Thus, Fn was sufficient to describe the fluid flow. Further, several combinations of independent variables were tested during the analysis and the effective combinations were included in the analysis to improve the correlation of the final form as shown in Table 6 and Eq. (7).

The coefficients for each independent variable can be rounded off so that the final form of the empirical equation can be written as follows;

$$Ln(Ct^2) = 7.13 + 191.36 \times Fn - 1.57 \times Ln(Ep) - 1.02 \times Ad - 6.55 \times Slr - 636 \times Ws + 2422 \times (Ws)^2 - 100.2 \times Fn \times Slr + 1.51 \times Ln(Ep) \times Slr + 193.16 \times Slr \times Ws \quad (7)$$

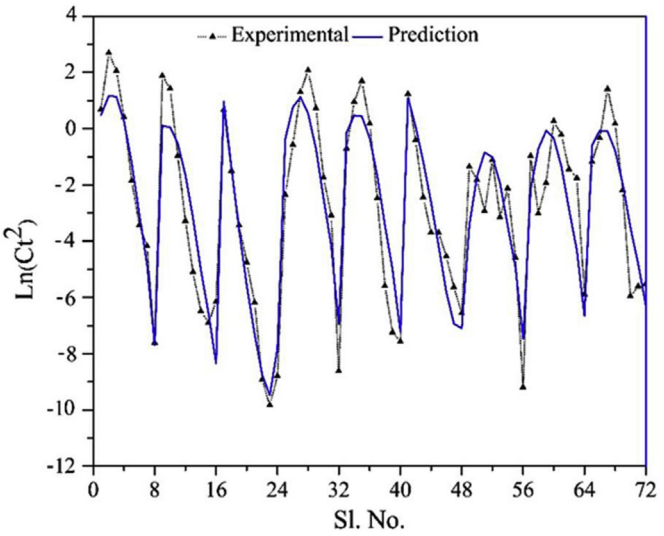

Fig. 8. Experimental results compared with the results obtained from the empirical formula.

Fig. 8 shows the comparison of the results between the experiment and the empirical formula. The comparison is shown on a log scale. Even though the distribution of the experimental results does not adhere to an easily defined mathematical form, the results obtained from the empirical formula could elicit a good agreement with the experimental results.

4. Verification

We derived an empirical formula as shown in Eq. (7), based on our experiments carried out in a wave flume. Where the water depth was restricted to 40 cm. As a solution, we have wave slope as an independent variable for the multiple regression analysis to include the effects of a change in water depth. Further, to validate our method, we carried out a model test with the same model set up in a wide tank (30 m long, 20 m wide, and 2.5 m deep) where the water was comparatively deeper. We used the same hydrofoil attached with an elastic plate of the length 'L2' and breadth 'B2'. Subsequently, we generated four regular incoming waves as shown in Table 7 and measured the thrust force using the same capacity load cell as mounted on the wave flume. The comparison of the results is displayed in Fig. 9 which shows a good agreement between the experimental and predicted results for the widetank. Therefore, the empirical formula could be useful for the thrust estimation of a passive flapping foil (NACA0015) regardless of any water depths, where the foil was attached to an elastic plate and incoming surface gravity waves excites the flapping motion of the foil using the vertical components of the wave orbital velocity.

Table 6
Results of regression analysis for the thrust generation of flapping foil.

	Coefficients	Standard Error	t Statistic	P-value	Lower 95%	Upper 95%
Intercept	7.13	1.76	4.06	0.00	3.62	10.64
Fn	191.36	37.87	5.05	0.00	115.66	267.05
Ln(Ep)	−1.57	0.32	−4.88	0.00	−2.21	−0.93
Ad	−1.02	0.27	−3.80	0.00	−1.56	−0.48
Slr	−6.55	2.52	−2.60	0.01	−11.58	−1.52
Ws	−635.99	102.49	−6.21	0.00	−840.86	−431.11
Ws^2	2422.10	606.51	3.99	0.00	1209.70	3634.50
Fn × Slr	−100.19	32.08	−3.12	0.00	−164.31	−36.07
Ln(Ep) × Slr	1.51	0.40	3.74	0.00	0.70	2.31
Slr × Ws	193.16	40.78	4.74	0.00	111.65	274.68

Table 7
Load cases for widetank experiments.

Load Case	H(cm)	ω (rad/s)	Wave Number (K)	Wave Slope (Ws)
1	2	4.63	2.18	0.0069
2	3	4.63	2.18	0.0104
3	2	9.24	8.72	0.0277
4	3	9.24	8.72	0.0416

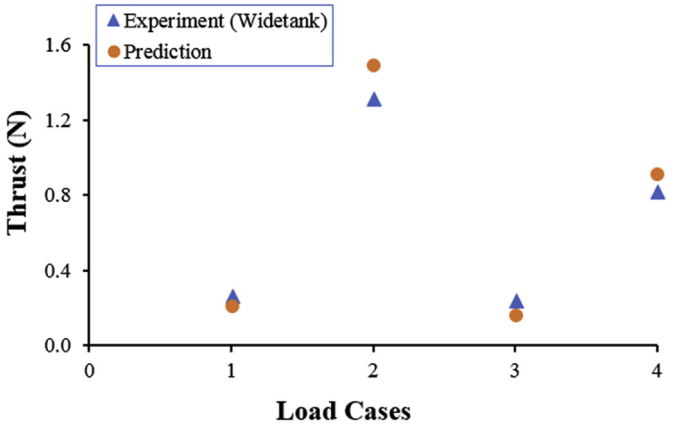

Fig. 9. Experimental results in widetank compared with the results obtained from the empirical formula.

5. Conclusion

In this study, thrust force generated by the flapping motion of a foil attached to an elastic plate in the presence of waves was investigated experimentally, whereby the foil could flap at a fixed location. Since our aim was to develop a stationkeeping system of a floater using flapping foils in waves, we did not allow the foil to drift during the experiments. It could only flap with the waves using wave energy. Based on the measurement of thrusts experimentally, an empirical equation used for the prediction of thrust generated by the flapping foil in regular waves is introduced. In addition, the effects of the water depth, length of elastic plate, and breadth of elastic plate on the thrust force were discussed in detail. Finally, the following conclusions were drawn based on this study.

1. The thrust forces of the flapping foil (NACA0015) attached to an elastic plate can be predicted using the empirical formula.
2. Elastic plates could be useful to design a very effective control system for the stationkeeping of a floater.

Acknowledgements

This work was supported by the Korea Institute of Energy Technology Evaluation and Planning and the Ministry of Trade, Industry and Energy of the Republic of Korea (No. 20184030202280) and Korea Electric Power Corporation (No: R18XA03).

References

Belibassakis, K.A., Filippas, E.S., Touboul, J., Rey, V., 2015. Hydrodynamic analysis of oscillating hydrofoils in waves and currents. Towar. Green Mar. Technol. Transp. 185–192.
Blondeaux, Paolo, Fornarelli, Francesco, G, L., 2005. Numerical experiments on flapping foils mimicking fish-like locomotion. Phys. Fluids 17. https://doi.org/10.1063/1.2131923.
Bøckmann, E., Steen, S., 2014. Experiments with actively pitch-controlled and spring-loaded oscillating foils. Appl. Ocean Res. 48, 227–235.
Evangelos, S.F., 2015. Augmenting ship propulsion in waves using flapping foils initially designed for roll stabilization. In: YSC 2015. 4th Int. Young Sci. Conf. Comput. Sci. Elsevier B. V., Athens, pp. 103–111.
Filippas, E.S., Belibassakis, K.A., 2014. Hydrodynamic analysis of flapping-foil thrusters operating beneath the free surface and in waves. Eng. Anal. Bound. Elem. 40, 47–59.
Fish, F.E., 2013. Advantages of natural propulsive systems. Mar. Technol. Soc. J. 47, 37–44.
Gause JA. Flexible Fin Propulsion Member and Vessels Incorporated Same. GB Patenet 1176559, 1966.
Hover, F.S., Haugsdal, Triantafyllou, M.S., 2004. Effect of angle of attack profiles in flapping foil propulsion. J. Fluid Struct. 19, 37–47. https://doi.org/10.1016/j.jfluidstructs.2003.10.003.
Isshiki, H., 1994. Wave energy utilization into ship propulsion by fins attached to a ship. Bull Soc Nav Archit Japan III, 508.
Jakobsen, E., 1981. The foilpropeller, wave power for propulsion. In: Second International Symposium on Wave & Tidal Energy. BHRA Fluid Engineering, pp. 363–369.
Lee, J., Park, Y.J., Cho, K.J., Kim, D., Kim, H.Y., 2017. Hydrodynamic advantages of a low aspect-ratio flapping foil. J. Fluid Struct. 71, 70–77. https://doi.org/10.1016/j.jfluidstructs.2017.03.006.
Hermann Linden. Improved combination with floating bodies, of fins adapted to effect their propulsion. GB Patent 14,630. Filed Aug. 1, 1895. Patented Jul. 18, 1896. GBD189514630 (A), n.d.
Liu, Z., Tian, F.B., Young, J., Lai, J.C.S., 2017. Flapping foil power generator performance enhanced with a spring-connected tail. Phys. Fluids 29. https://doi.org/10.1063/1.4998202.
Liu, Peng, Liu, Yebao, Huang, Shuling, Jianfeng Zhao, Y.S., 2018. Effects of regular waves on propulsion performance of flexible flapping foil. Appl. Sci. 8, 934. https://doi.org/10.3390/app8060934.
Prempraneerach, P., Hover, F.S., Triantafyllou, M.S., 2003. The effect of chord wise flexibility on the thrust and efficiency of a flapping foil. In: Int Symp Unmanned Untethered Submers Technol.
Read, D.A., Hover, F.S., Triantafyllou, M.S., 2003. Forces on oscillating foils for propulsion and maneuvering. J. Fluid Struct. 17, 163–183. https://doi.org/10.1016/S0889-9746(02)00115-9.
Kazi Shah Nawaz Ripon, JMKG. Optimizing bio-inspired propulsion system using genetic algorithm. Comput. Intell. (SSCI), 2017 IEEE Symp. Ser., Honolulu, HI, USA: n.d. doi:10.1109/SSCI.2017.8285175.
Silva, L.W.A.D., Yamaguchi, H., 2012. Numerical study on active wave devouring propulsion. J. Mar. Sci. Technol. 17, 261–275.
Terao, Y., 1982. A floating structure which moves towards the waves (possibility of wave devouring propulsion. J Kansai Soc Nav Archit Japan 51–54.
Ulysses S. Harkson; san mateo; WATER CRAFT HAVING HYDROPLANES, 2,821,948 United States patent office, claim. (CI. 114-66.5), 1958.
Xie, Y.-H., Jiang, W., Lü, K., Zhang, D., 2016. Review on research of flapping foil for power generation from flow energy. Zhongguo Dianji Gongcheng Xuebao/Proceedings Chinese Soc Electr Eng 36, 5564–5575. https://doi.org/10.13334/j.0258-8013.pcsee.160797.
Xu, G.D., Duan, W.Y., Zhou, B.Z., 2017. Propulsion of an active flapping foil in heading waves of deep water. Eng. Anal. Bound. Elem. 84, 63–76. https://doi.org/10.1016/j.enganabound.2017.08.014.
Yu, J., Tan, M., Wang, S., Chen, E., 2004. Development of a biomimetic robotic fish and its control algorithm. IEEE Trans Syst Man Cybern 34, 1789–1810.
Zhou, K., Liu, J., Chen, W., 2017. Study on the hydrodynamic performance of typical underwater bionic foils with spanwise flexibility. Appl. Sci. 7, 1120.